William Flanders

Using HI Observations to Test Ultra-Light Axion Dark Matter

Submitted in accordance with the
requirements for completion of the degree of
Bachelor of Science in Astrophysics

submitted to

Haverford College

Advisors
Prof. Karen Masters
Prof. Daniel Grin

370 Lancaster Ave
Haverford PA 19041

May 2023

Abstract

The ΛCDM model predicts a large population of low-mass galactic halos. This prediction is often in contrast with observational distributions of galactic halos, putting the number density of such halos at a much smaller value than is theoretically expected. In contrast, ULA models create suppression in the growth of these small scale populations and thus are a plausible solution for the discrepancy between theoretical and observational results. In this thesis, we use data from mock 21cm neutral hydrogen (HI) surveys based on real life survey detection limits. The mock surveys were conducted in simulated universes that employed CDM and ULA dark matter models. We then construct mock HI Width Functions (HIWFs) as probes to test ULA dark matter. We find that our mock HIWFs are not robust enough to definitively test the ULA as a viable dark matter model.

1 Introduction

1.1 Dark Matter and the ΛCDM Model

In the late 1930's, astronomers noticed that estimates for the virial, or gravitationally bound, mass in galaxies were orders of magnitude greater than any mass estimate from the galaxy's luminosities (i.e. from just looking at the galaxy optically and estimating the mass in stars which create that light, Zwicky, 1937). Then, in the late 1970's, Vera Rubin (along with Kent Ford) discovered that galaxy rotation curves defied expectation. The material at the edge of a galaxy appeared to be rotating with circular velocity just as fast as material towards the center (Rubin et al., 1978) as shown in Figure 1.1. This was a clear departure from the explanation that typical Newtonian mechanics provides and that we observe in the solar system in that orbital velocity decreases with the square root of the distance between gravitationally bound objects. Since then, further research has revealed that the amount of visibly available matter present in galaxies is no where near enough to account for the additional gravitational potential required to keep the edge of the galaxy rotating at the same speed as its center (Zwicky, 1933; Smith, 1936) and thus, the discovery of dark matter in galaxies. Very little is understood about dark matter other than it has gravitating mass and plays a key role in cosmological phenomena, galactic dynamics and structure (Frenk et al., 1996; Dekel and Silk, 1986), it only appears to interact with baryonic (normal, everyday) matter gravitationally, it seems to constitute 96% of the total gravitating matter of the universe (Bennett et al., 2003), and it resides in halos surrounding galaxies and other large scale structures (Navarro, 1996).

Many attempts have been made to identify what dark matter exactly is. The most widely accepted cosmological model is the ΛCDM model. Λ is the cosmological constant, in Einstein's Theory of General Relativity, and represents the accelerated expansion of the universe. CDM is an acronym for cold dark matter and is one of the more popular theories that could explain the mysterious substance. Temperature as an adjective here describes the average speeds at which a typical particle of dark matter would be travelling at relative to the speed of light. Hot dark matter (HDM) is a model that describes a particle that moves with relativistic speeds (speeds close to the speed of light) while CDM is a similar such model but with speeds far less than the speed of light. There are many advantages to using a CDM model as opposed to a HDM one. The most notable is that HDM smears

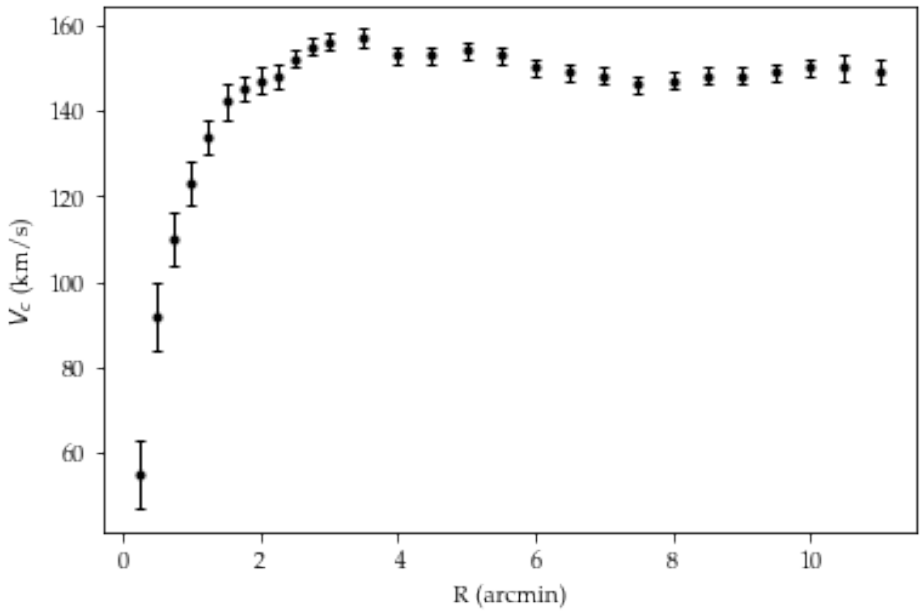

Figure 1.1: Galaxy NGC3198's flat rotation curve. The plot shows the circular velocity as a function of radius and how the circular velocity appears constant as radius increases (Begeman, 1989).

out the large scale structure of galaxies (Davis et al., 1992). This is in direct contrast to observations made today and thus HDM isn't considered a viable model. On the other hand, simulations of CDM predict galaxy distributions close to current observations (White et al., 1987). Other theories of dark matter include self-interacting dark matter (SDIM, Spergel and Steinhardt, 2000), and warm dark matter (WDM, Maio and Viel, 2015). The nature and reason for scientists proposing these models as alternatives to CDM vary, usually due to some shortfall of ΛCDM (Young, 2017).

Popular CDM theories predict a hypothetical weakly interacting massive particle (WIMP) as a relic dark matter particle from the early universe. WIMPs are characterized by their large masses and inability to interact at any scale larger than the weak force. Current cosmological models predict that the early universe was extremely dense and hot. At these sufficiently high temperatures, all particles of the standard model were in thermal equilibrium. This relic dark matter particle would be forming from the particle bath and then annihilating with its antiparticle pair, forming lighter particles. When the universe eventually expanded and cooled, the particle bath would no longer be energetic enough to form new dark matter particles and so all dark matter production would cease. Dark matter annihilation, however, would continue and the dark matter particle's number density would begin to decrease. Eventually, the expansion of the universe would forbid

this process too, as the particle-antiparticle pairs could no longer find each other, and dark matter will have frozen out with a constant number density. Particles that have larger interaction cross sections will have annihilated for longer and therefore have a smaller number density. Based on current measurements of the abundance of dark matter, it would need to have a interaction cross section no larger than that for the weak force, thereby seemingly supporting a WIMP CDM theory.

Other popular CDM candidates are massive, compact, halo objects (MACHOs), and the axion, which will be the focus of this paper. A MACHO model predicts that large objects, like black holes or brown dwarfs, comprise the dark matter halo. These large objects would have considerable gravitational potentials but aren't bright enough that scientists could be able to detect them making them potential dark matter candidates. MACHOs have lost favor and have been nearly totally ruled out as a possible candidate (Carr et al., 2010; Peter, 2012). Axions, which as a particle of dark matter have been nicknamed fuzzy dark matter (FDM), have increasingly become more popular and the nature of such axionic dark matter will be discussed in more detail in Section 1.3. Regardless of the exact nature of dark matter, ΛCDM's success can't be overstated. The model has successfully predicted a wide range of observations, from the statistics of weak gravitational lensing (Brouwer et al., 2016) to the polarization of the CMB (Ade et al., 2016).

In spite of all the success, ΛCDM still falls short in certain areas where predictions fail to match observation. One such shortfall has been dubbed the Missing Satellites Problem (MSP) the nature of which will be discussed in further detail in Section 1.2. In attempting to resolve a problem, a theory would ideally need to be able to retain all the success of ΛCDM and its core behavior before potentially expanding on it in a new direction. While seeming like a fairly limiting constraint, the alternatives to ΛCDM are actually quite plentiful, namely positing WDM to solve small-scale CDM crises in the early universe (Maio and Viel, 2015), and SIDM to solve the famous cuspy-core problem (Spergel and Steinhardt, 2000).

In this thesis, I look to consider one such alternative to ΛCDM where very low mass, or ultra-light, axions constitute dark matter in an attempt to solve the MSP. The nature of the MSP, how it arises, and the observational evidence against standard ΛCDM will be discussed in Section 1.2. The physics of axions and how they could potentially be a dark matter particle will be discussed in Section 1.3. Simulation data and methods will be discussed in Section 2. Outputs and results are shown in Section 3 and their broader implications are discussed in Section 4.

1.2 HI Surveys and the Missing Satellites Problem

1.2.1 HI Surveys and the HI Width Function as a Probe

HI, or neutral, atomic hydrogen, is the raw material that ultimately forms stars (Zhou et al., 2018). As such, it plays an extremely important role in galaxy formation and evolution. What makes HI so useful as a tool in astronomy is the emission line that it produces when it undergoes a quantum state change due to the spin of its electron flipping. This emission line has a wavelength of 21cm due to the energy split of the quantum states. This puts the line firmly in the radio wave range of light and as a result is capable of easily passing through the Earth's atmosphere. HI mass can be measured since HI is optically thin, and so mass is proportional to flux. More so, if the gas is in dynamic equilibrium, i.e its bulk motion is a result of the circular motion of the galaxy and not due to extenuating phenomena (like a galaxy merger), the width of the emission line due to Doppler broadening can be used to calculate the galaxy's rotational velocity since HI spatially extends far enough out to the flat portion of a galaxy's rotation curve. This in combination with an assumed or estimated size, can be used to calculate the galaxy's virial mass (Yu et al., 2020). HI surveys can directly measure large patches of sky to construct catalogues containing thousands of galaxies and their HI profiles. For example, the Arecibo Legacy Fast ALFA survey (ALFALFA) catalog contains 31500 extragalactic HI line sources and covers a sky area of 7074 square degrees (Haynes et al., 2018).

Given dark matter's elusive nature, methods of measurement and detection usually come in the form of indirect detection. As previously discussed, dark matter plays a key role in galaxy formation and evolution. Therefore, HI surveys can be used to construct various statistical tools that can probe and test dark matter models at extragalactic scales. One such tool is the HI mass function (HIMF), which describes the volume number density of galactic HI halos of a given HI mass. HIMFs are effective probes (Garland et al., 2024; Jones et al., 2018; Zwaan et al., 2005) for how dark matter affects structure formation at varying scales. In a similar vein, an HI velocity width function (HIWF) can be constructed which, like the HIMF, describes the volume number density of galactic HI halos but for a given HI velocity width to similarly probe galactic structure formation at low and high scales. While the HIWF doesn't directly represent the distribution of any actual fundamental galaxy property (unlike HI mass), it can still serve as a powerful tool to compare simulated data against theoretical expectations for HI surveys and will be the focus of this paper.

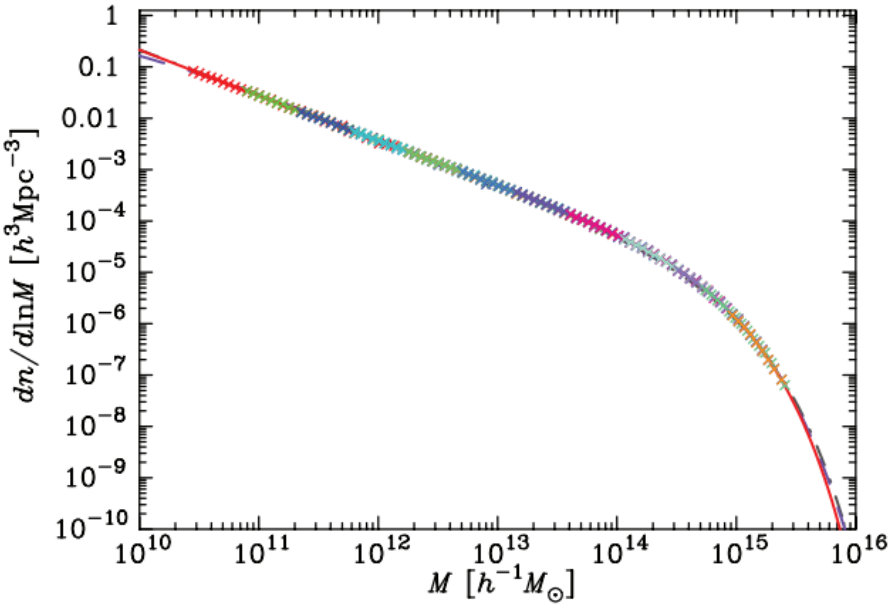

Figure 1.2: The halo mass function for sixteen simulated ΛCDM universes (Warren et al., 2006). Each simulation is in a different color. The Warren fit (Warren et al., 2006) is a solid red line, the Jenkins fit (Jenkins et al., 2001) is a dashed purple line, and the Sheth-Tormen fit (Sheth and Tormen, 2002) is a dark gray dot-dashed line.

1.2.2 The Missing Satellites Problem

A consequence of CDM is that structure forms ground up, first from small scales to larger scales. This sort of formation process is in-line with current cosmological models and is part of the reason why CDM is favored over HDM (which assumes that structure forms first from large scale to smaller scales). For a CDM model, objects in the universe would collapse under their own self gravity, before merging to form larger scale structures like galaxies. Therefore, it would be expected that there is a large number of low-mass dark matter halos as these would be the first in the chain to be produced. More specifically, the number density of dark matter halos as a function of their virial mass is described by a dark matter, or halo, mass function. Its been analytically predicted that the halo mass function (HMF) behaves as a power law with an exponent of $\alpha \approx -1.9$ at low halo masses (Sheth and Tormen, 2002; Press and Schechter, 1974). This has been confirmed by CDM N-body simulations (Warren et al., 2006; Boylan-Kolchin et al., 2009) as seen in Figure 1.2. The HMF predicts a large number of low-mass satellite halos for every Milky Way sized galaxy. Herein lies the problem; observational distributions paint a much shallower picture. These observational distributions similarly behave as a power law but with an

exponent of $\alpha \approx -1.3$ meaning not nearly as many satellites as predicted thus earning the name of the "missing satellites problem" (Klypin et al., 1999). This can be shown explicitly by comparing data from large HI (neutral atomic hydrogen) surveys and results from CDM simulations as seen in Figure 1.3.

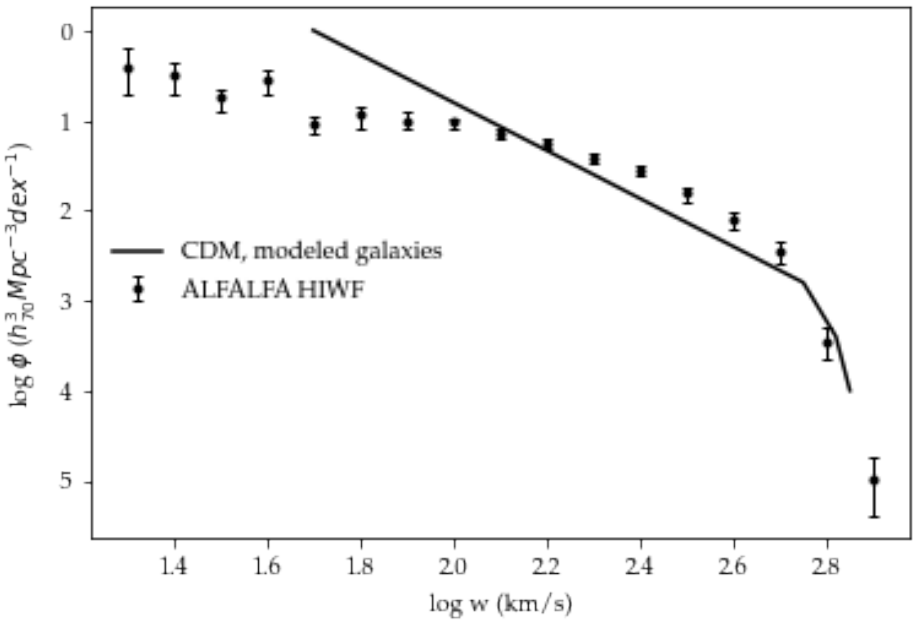

Figure 1.3: Data points with error show the ALFALFA HIWF from (Papastergis et al., 2011). The solid line represents the WF of a modeled galaxy populations corresponding to the CDM simulation of (Zavala et al., 2009). Note the discrepancy in growth rate of small HI halos between CDM modeled populations and observational populations in the low width range.

This observational discrepancy can be likely be attributed to either i.) a problem with standard CDM simulations, likely due to an inadequate DM model or ii.) improper comparison of simulated halos with observed galaxies due to either a problem with modeling of corresponding baryonic content or incorrect interpretation of HI linewidths as maximum rotational velocities (Papastergis et al., 2011).

In this thesis, I will consider ways to investigate if i.) could be the possible root cause. A possible solution would be to consider the ultra-light axion (ULA) as a candidate particle for dark matter. The details of the ULA as a possible model for dark matter will be discussed in the next section.

1.3 Axion Cosmology

1.3.1 Ultra-Light Axions

For clarity, "axion" in physics can take on multiple meanings. In general, axions can be broadly defined as a light pseudoscalar field and are used in many different disciplines as a sort of fix-it particle. The original quantum chromodynamics axion, called the Peccei-Quinn-Weinberg-Wilczek (PQWW) axion, was developed as a solution to the Strong CP problem (Peccei and Quinn, 1977). Other QCD axion solutions were also developed to solve miscellaneous problems including the Kim-Shifman-Vainshtein-Zakharov (KSVZ) axion (Kim, 1979; Shifman et al., 1980) and the Dine-Fischler-Srednicki-Zhitnitsky (DFSZ) axion (Dine et al., 1981; Zhitnitskii, 1980).

In the case of the ULA, the mass range considered in this thesis will be

$$10^{-24}eV \leq m_a \leq 10^{-20}eV. \tag{1.1}$$

The ULA's decay constant, $f_a \approx 10^{16}GeV$, is defined as the energy scale at which the particle is able to acquire mass (i.e. it is the scale at which Pecci-Quinn Symmetry is broken).

In the very early, hot, and dense universe, it is hypothesized that a period of extremely rapid expansion occurred, called inflation, 10^{-36} seconds after the Big Bang (BB) and lasted until 10^{-33} seconds after BB where the universe grew by a factor of at least 10^{26}. The temperature of the Universe during inflation is given by the Gibbons-Hawking temperature

$$T_I = \frac{H_I}{2\pi} \tag{1.2}$$

where H_I is the inflationary Hubble scale (Gibbons and Hawking, 1977). It has been shown that with current measurements of the tensor-to-scalar ratio, r_T, which is defined as the ratio of tensor perturbations (primordial gravitational waves) to scalar perturbations (what are observed as temperature fluctuations in the Cosmic Microwave Background (CMB) today), the inflationary temperature is constrained to approximately

$$\frac{H_I}{2\pi} < 1.4 \times 10^{13}GeV, \tag{1.3}$$

(Ade et al., 2015). Because $f_a > \frac{H_I}{2\pi}$, PQ symmetry is broken during inflation (Marsh, 2016). As a result, causally disconnected patches with different values of $\theta_{PQ} = \frac{\phi}{f_a}$ are generated, where ϕ is the pseudoscalar axion field. However, rapid inflationary expansion stretches each patch of θ_{PQ} such that our current Hubble volume, or the region of space

surrounding an observer where objects outside of the region recede at a rate faster than light, began with a single uniform value of θ_{PQ}. The initial value of θ_{PQ} is completely random and is drawn from a uniform distribution (Marsh, 2016).

There are two mechanisms for the generation of fluctuations in θ_{PQ} (these fluctuations seed structure formation via axionic dark matter). The first are via adiabatic fluctuations, or patches where θ_{PQ} might vary locally, but the overall density remains the same. The second is a result of isocurvature perturbations. When PQ symmetry is broken during inflation, we have $m_a << H_I$ and the axion exists as a massless field. All massless fields in de Sitter space (mathematical description of space without matter) experience quantum fluctuations with amplitude

$$\delta\phi = \frac{H_I}{2\pi}. \tag{1.4}$$

The production of a relic ULA population can be attributed to i.) parent particle decay, ii.) topological defect decay, iii.) thermal production from radiation bath, and iv.) vacuum realighment (Marsh, 2016).

The axion field potential can be written approximately as

$$V(\phi) \approx \frac{1}{2} m_a^2 \phi^2, \tag{1.5}$$

which is the dominant term of a Taylor approximation thats valid if only small, $\phi < f_a$ displacements from the potential minimum are considered (Winch et al., 2023).

The homogeneous equation of motion for the axion field is described by

$$\ddot{\phi} + 3H\dot{\phi} + m_a^2\phi = 0, \tag{1.6}$$

which is the equation of a simple harmonic oscillator.

The axion field energy density and pressure is given by

$$\rho_a = \frac{1}{2}\dot{\phi}^2 + \frac{1}{2} m_a^2 \phi^2, \tag{1.7}$$

and

$$P_a = \frac{1}{2}\dot{\phi}^2 - \frac{1}{2} m_a^2 \phi^2, \tag{1.8}$$

respectively.

At later times, when $H << \frac{m_a}{3}$, ϕ begins to coherently oscillate, with cycle averaged density scaling as $\langle \rho_a \rangle \propto a^{-3}$ (Turner, 1983). This has the same time dependence as matter and for $m_a \geq 10^{-27} eV$, the transition would take place after the radiation epoch in the

universe. As a result, ULAs would behave as matter and contribute to the dark matter density of the universe (Garland et al., 2024).

The de Broglie wavelength, the length scale at which particles begin to behave like waves, of the ULA is given by

$$\lambda_a = \frac{1}{m_a v_a}, \tag{1.9}$$

where v_a is the axion velocity with respect to the Hubble flow, or the flow of galaxies due to the expansion of the universe. Because m_a is exceptionally small, λ_a is remarkably large.

It is useful then, if not ideal, to model the axion field as a fluid. This is a consequence of considering the quadratic potential well from Equation 1.3.1. As a result, axion perturbations can be conducted in a fluid treatment. It is possible to construct a scale-dependent sound speed given by

$$c_s^2 \approx \frac{k^2/(4m_a^2a^2)}{1 + k^2/(4m_a^2a^2)}, \tag{1.10}$$

where k is the wavenumber and a is the cosmological scale factor(Hwang and Noh, 2009; Passaglia and Hu, 2022).

At small scales, $k >> m_a a$, and thus $c_s \to 1$, while on large scales, $c_s \to 0$, thereby recovering CDM behavior.

A direct result is that fractional ULA density fluctuations, δ_a obey the usual 2nd order equation for Jeans instability, the critical density at which self-gravitational collapse is assured (Hu et al., 2000) namely,

$$\ddot{\delta}_a + 2H\dot{\delta}_a + \left[\frac{k^2c_s^2}{a^2} - 4\pi G\rho_a\right] = 0, \tag{1.11}$$

where perturbation growth for wavenumbers $k > k_J$ beyond the comoving ULA Jeans scale is prevented due to acoustic pressure. More specifically, at any scale less than k_J, the uncertainty principle from wave mechanics prevents confining the the fluid to a more defined position via gravitational collapse without conferring it the additional momentum it would need to escape collapse (Hu et al., 2000).

Thus, the abundance of dark matter halos for small scales is strongly suppressed where

$$M \leq M_j(z) = \frac{4\pi}{3}200r_J^3\rho_0(z), \tag{1.12}$$

where $r_J = \frac{2\pi}{k_J}$ is the Jeans scale and $\rho_0(z)$ is the mean cosmic density at redshift z (Marsh, 2016).

The ULA as the dark matter particle suppresses small scale halo overproduction for the same reason that the hydrogen atom is stable. Its extremely large de Broglie wavelength means it behaves like a wave at astronomical distances and so any attempt to gravitationally collapse below this scale is met with the uncertainty principle. At scales larger than the particle's de Broglie wavelength, halos can form as the axion fluid is able to gravitationally collapse and expected CDM behavior is recovered. This makes the ULA a promising candidate to solve the MSP.

2 Methodology

2.1 HI Data Collection and Processing

As introduced in Section 1.2.1, large HI surveys provide catalogues with plentiful galaxy HI global profiles that can then be used to construct valuable statistics like the HIWF. These surveys usually employ a pipeline to handle the collection and processing of thousands of galaxies and radio sources. These surveys rely on large telescopes, like the Arecibo Telescope in Puerto Rico or the Australian Square Kilometer Array Pathfinder (ASKAP) Telescope in Australia, to scan large swathes of sky and collect thousands of radio sources. The resulting HI profiles are then analyzed, cleaned, and fitted to approximate useful galaxy parameters like total HI mass content or line width.

The wavelength of light that HI emits is always 21cm due to the quantum mechanical nature of the hydrogen atom. Since nearly all galaxies are moving away from us, the entire profile will be redshifted. Therefore, any measurements gathered from the profile will be measured relative to some mean recessional velocity of the galaxy. Additionally, because of the galaxy's rotation, the wavelengths of light that are actually observed can be shifted longer or shorter than 21cm. This is because of the Doppler effect (Beals, 1936). The half of the galaxy that is rotating away from Earth will shift red (or have longer wavelengths) and the half that is rotating towards Earth will shift blue (or have shorter wavelengths). The result is a characteristic double horned profile as seen in Figure 2.1.

The universe, as well as the telescope used to observe, are contain inherent sources of noise that can slip into samples. Surveys will employ a data cleaning pipeline that measures and separates the noise from the signal. Samples with poor signal to noise ratios are often discarded in final catalogues as galaxy statistics can't be reliable inferred from the noise-shrouded signal. The profiles can then be functionally fit and quantities like the total HI mass content can be derived by integrating over the area under the signal. The velocity width of a profile, W or W_{50}, can be calculated by measuring the full width of the signal at half the maximum output (FWHM). From there, an inclination, or the galaxy's tilt relative to our line of sight, correction can be applied to W to recover the rotational velocity of the galaxy, V_{rot}.

Naturally, there is a limit to the detectability of a given galaxy, largely governed by a telescope's sensitivity and survey's scope. For this paper, we will be utilizing a mock

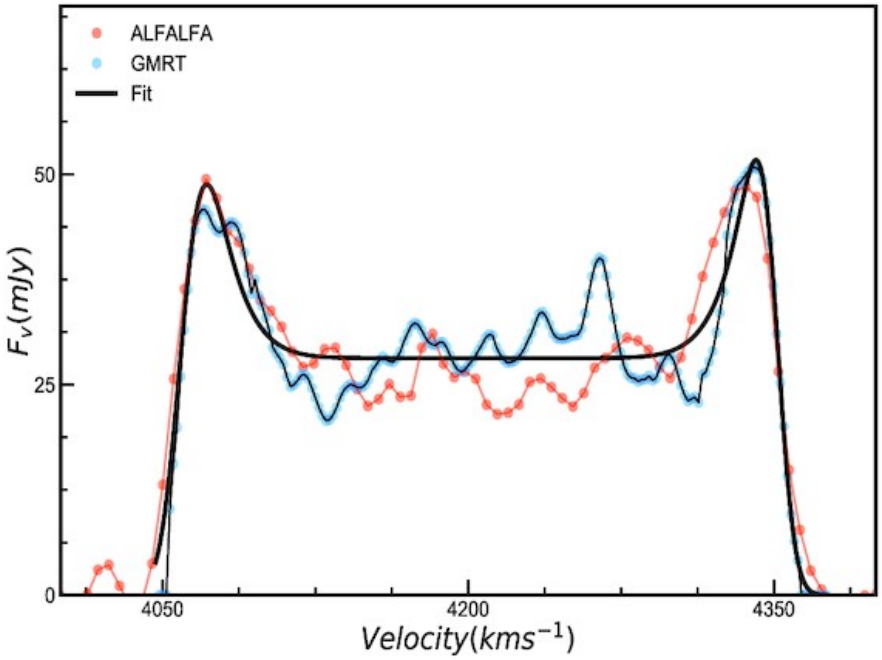

Figure 2.1: A fitted radio profile of FGC 1440 (Aditya et al., 2022). The red line is data that comes from ALFALFA, the blue line is data that comes from the Giant Meterwave Radio Telescope (GMRT) in India. Note the double horned shape as a result of Doppler broadening. The profile is centered at 4200 kms^{-1}, indicating the redshift of the galaxy as a result of its recessional motion from the Milky Way.

survey dataset generated by (Garland et al., 2024) where the detectability limits of the ALFALFA (Haynes et al., 2018) and WALLABY (Koribalski et al., 2020) (Westmeier et al., 2022) surveys are used to conduct mock observations of simulated data that posits the ultralight axion as the dark matter particle. These mock observations form a simulated catalogue of galaxy HI detections, similar to real HI surveys. An HIWF can then be constructed to compare varying axionic dark matter cosmologies.

2.2 Halo Simulations and Mock HI Surveys

The dataset generated by (Garland et al., 2024) consists of six different spherical 100 Mpc universes that are populated with dark matter halos. One of these universe's halo population follows the halo mass function (HMF) for CDM, and the other five follow the HMF for the ULA model with the mass of the axion varying between each universe. The ULA HMF is well described by a Sheth-Tormen fit (Sheth and Tormen, 2002) given by

$$f(v) = A\sqrt{\frac{a}{2\pi}}v\left|(1+av^2)^{-p}\right|\exp(-av^2/2), \tag{2.1}$$

where $A = 0.322$, $a = 0.707$, $p = 0.3$, and $v = \delta_{crit}/\sigma(M) = G(M)v_{CDM}$ (Marsh, 2016) where δ_{crit} is the mass-dependent collapse threshold. Figure 2.2 shows the output of numerical simulations from (Du et al., 2016) of HMFs for different axion masses as well as CDM.

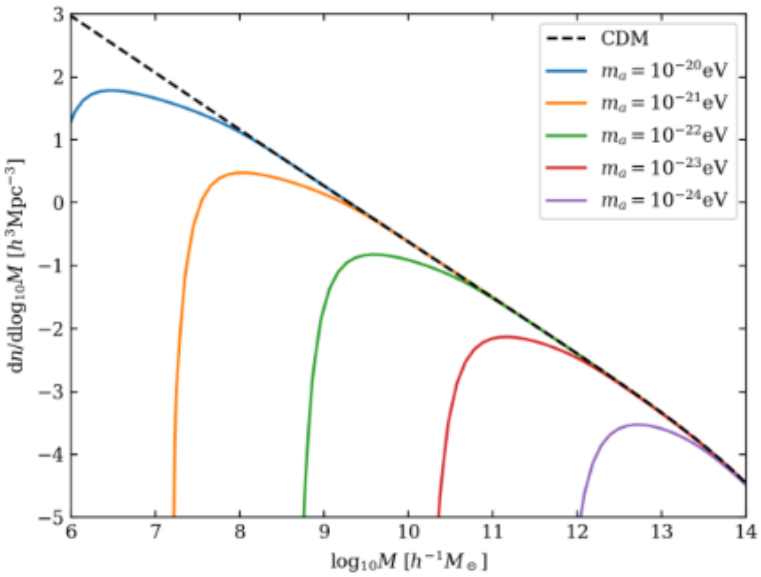

Figure 2.2: HMFs for various axion masses as well as CDM from (Du et al., 2016). Note the suppression in the number density of halos at the low mass regime for ULA HMFs.

For each halo, the authors randomly assigned a position within the universe as well as an inclination angle, i, that was sampled from a uniform $\sin i$ distribution. They assigned HI mass, M_{HI}, to each halo following the relationship

$$M_{HI}(M_h) = M_0\left(\frac{M_h}{M_{min}}\right)^a \exp\left(\frac{-M_{min}}{M_h}\right)^{0.35}, \tag{2.2}$$

where $M_0 = (4.3 \pm 1.1) \times 10^{10}h^{-1}M_\odot$, $a = 0.24 \pm 0.05$, and $M_{min} = (2.0 \pm 0.6) \times 10^{12}h^{-1}M_\odot$. Equation 2.2 is taken from Villaescusa-Navarro et al. (2018) which used output from Illustris TNG (Nelson et al., 2021), a smooth particle hydrodynamics simulation

with a $75h^{-1}$Mpc box size. Disc rotation velocities are then assigned following a v_{flat} - M_h relationship found by Katz et al. (2019) where

$$V_{flat} = 10^{-B/A} M_h^{1/A}, \tag{2.3}$$

where $A = 2.902 \pm 0.138$ and $B = 5.439 \pm 0.292$. The observed HI line width, that is the line width that would be seen by a telescope on Earth, can be calculated from

$$W = 2V_{flat} \sin i. \tag{2.4}$$

The authors then performed mock detections to generate a catalogue similar to what would be produced on Earth given the detection limits of the surveys. For ALFALFA for Code 1 detections, which is defined as detections with a signal to noise ratio of at least 6.5, Haynes et al. (2018) cites a 90% completeness limit of

$$\log S_{21,90\%,\text{Code 1}} = \begin{cases} 0.5 \log W_{50} - 1.14, & \log W_{50} \leq 2.5 \\ \log W_{50} - 2.39, & \log W_{50} \geq 2.5 \end{cases} \tag{2.5}$$

where S_{21} is the total integrated flux. For WALLABY, Koribalski et al. (2020) estimates a 5σ M_{HI} detection limit for a source measured by a single beam as

$$M_{HI}[M_\odot] = \left(3901 W^{0.493}\right) D^2. \tag{2.6}$$

Garland et al. (2024) classifies any halo that satisfies these detection limits, that is possesses a flux greater than the limit, as "detected" for the corresponding mock survey.

The output of the simulation and mock observations is six fits files, one for each universe, as described in Table 2.1.

The construction of mock HIWFs using this dataset is discussed in the next section.

2.3 HIWF Construction

The HIWF describes the volume number density of galactic HI halos for a given velocity width. Therefore to construct it, one should logarithmically bin by velocity width and count the number of halos in each bin. However, halos with larger velocity widths are more detectable at greater distances than halos with smaller widths. Without taking this effect into account, the HIWF would overestimate the number of large velocity width halos. A solution is to weight each halo by the inverse of the maximum volume within which each halo could be observed within the survey, hence a *volume* number density. This is the core idea behind the $1/V_{max}$ method (Schmidt, 1968). More specifically, the maximum

Column Name	Units
dist	$\mathrm{Mpc}h^{-1}$
phi	rad
theta	rad
inc	deg
v_{rec}	$\mathrm{km}s^{-1}$
v_{rot}	$\mathrm{km}s^{-1}$
m_{HI}	$\mathrm{M}_{\odot}h^{-1}$
m_{h}	$\mathrm{M}_{\odot}h^{-1}$
alfalfa	bool
wallaby	bool

Table 2.1: Output of the simulation and mock observations. The 'alfalfa' and 'wallaby' columns are booleans that return true if the halo is detectable in the respective survey, and false otherwise.

volume at which each halo can be observed within a given bin, V_{max}, is calculated, before summing its reciprocals,

$$\phi_k = \sum_i \frac{1}{V_{max,i}}, \tag{2.7}$$

where ϕ_k is the halo volume number density and i is a given halo of a given velocity width bin, k. Halos with larger velocity widths will have greater maximum volume at which they can be observed, and so by weighting each halo by the reciprocal of the maximum detectable volume, any overestimation of larger width halos is minimized.

Because the simulated data is spatially homogeneous, no additional corrections for large scale structure, like an over dense halo region of space, or distance errors is required (Masters et al., 2004; Zwaan et al., 2005; Papastergis et al., 2011; Garland et al., 2024).

To calculate the maximum volume at which a given halo can be detected, the following relationship,

$$M_{HI} = \left(2.356 \times 10^5\right) D^2 S_{21}, \tag{2.8}$$

can be inverted to calculate a given halo's total HI flux content since M_{HI} and D is provided by the mock catalogue. Along with with the sensitivity limits given by Equation 2.5, the maximum distance at which the halo is detectable can be calculated, and as a result the maximum volume.

Similarly, for WALLABY (Koribalski et al., 2020), Equation 2.6 corresponds to a sensitivity of $M_{HI} = 5.3 \times 10^8 M_{\odot}$ at a distance of 100 Mpc assuming typical width, W = 250

kms^{-1}. This can then be used to calculate maximum detectable distance and subsequently maximum volume.

V_{max} weighting was performed for both surveys for all six universes resulting in twelve HIWFs for which to analyze ULA models. Furthermore, an additional "ideal" survey HIWF is constructed for each universe which posits that all halos are observable, and therefore the maximum detectable volume for any given galaxy is simply the size of the universe. Such a survey would then represent the "true" underlying distribution of halos across velocity width bins and provide an ideal model for which to compare the mock ALFALFA and WALLABY HIWFs against (Garland et al., 2024).

Additionally, the deviation between ULA and CDM model is quantified as

$$N\sigma_k = (\phi_{obs,k} - \phi_{CDM,k})/\sigma_{obs,k}, \tag{2.9}$$

where ϕ_{obs} is the given observed ULA density, ϕ_{CDM} is the given observed CDM density, and σ_{obs} is the Poisson counting error associated with ϕ_{obs}, all for a given velocity width bin, k.

3 Results

The output of the mock HIWFs, in logarithmic bins, is shown in Figure 3.1. Each panel represents a 100 Mpc universe with a corresponding dark matter particle, either CDM or a ULA with mass $m_a = 10^{-20}, 10^{-21}, 10^{-22}, 10^{-23}$, or 10^{-24} eV. As mentioned previously, each mock HIWF has been weighted using the V_{max} method, and the ideal survey (in orange) represents a survey where all halos are detectable; thus representing the true HIWF for a given universe not restricted by survey detection limits.

The mock HIWFs in Figure 3.1 show a clear linear growth in number density that is consistent with CDM models, until the observational surveys and ideal survey diverge at a width cutoff. Interestingly, the mock HIWFs appear to inherit the general linear shape of the HMFs, as seen in Figure 2.2, as opposed to the expected Schechter shape that the actual ALFAFA HIWF displays, as seen in Figure 1.3. Most notably, the characteristic "knee" that is expected at $\log w \approx 2.6$ is entirely missing. Furthermore, counts for bins in the lower width regime for ALFALFA are several orders of magnitude greater than values Papastergis et al. (2011) cite for their HIWF. While the mock universe has roughly four times as many total data points as Papastergis et al. (2011), this still doesn't account for the total over-observing of low width halos. Both of these discrepancies are discussed in more detail in Section 4.

Figures 3.2 and 3.3, binned logarithmically, are heat maps illustrating the deviations between mock HIWFs ULA models and the simulated CDM HIWF, as given by Equation 2.9. Slashed regions represent bins that have observational detections less than or equal to 5. Figures 3.2 and 3.3 show low deviation between CDM and universes with axion masses $m_a = 10^{-20}$ and 10^{-21} eV. These behaviors are discussed in more detail in Section 4.

Since ALFALFA is completed (Haynes et al., 2018), an observational HIWF can be constructed (Papastergis et al., 2011) in which simulated data can be compared against. This is illustrated in Figure 3.4.

Further analysis of these results are discussed in more detail in Section 4.

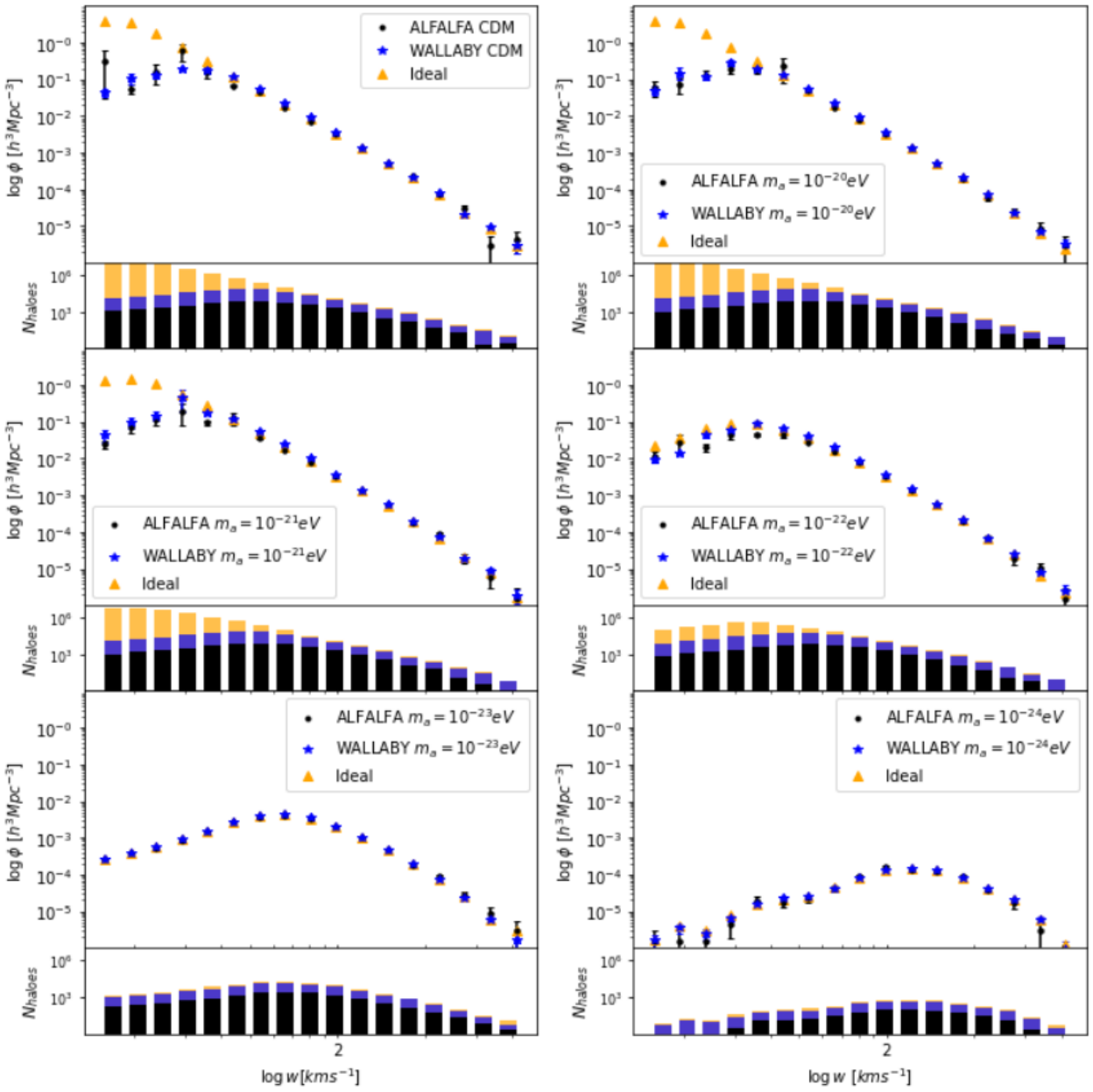

Figure 3.1: Mock HIWFs for six different 100 Mpc universes. Each universe varies by dark matter particle, specifically it is either CDM or a ULA with mass $m_a = 10^{-20}, 10^{-21}, 10^{-22}, 10^{-23}$, or 10^{-24} eV. Orange triangles represent an ideal survey where all halos are observable and represents the true HIWF. Black circles and blue stars represent HIWFs that would be detected by ALFALFA and WALLABY respectively. Error bars correspond to 1σ Poisson errors. The histograms for each plot shows the observed halo counts in each bin for each respective survey.

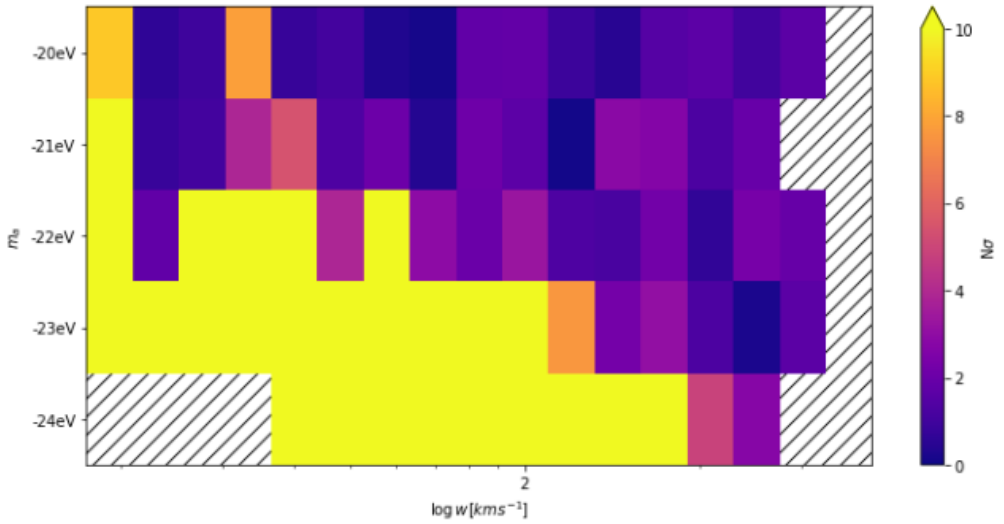

Figure 3.2: Deviations between ALFALFA and CDM HIWFs, in factors of observational error. Slashed regions indicate bins that have counts ≤ 5. Universes with ULA mass $m_a = 10^{-20}$ and 10^{-21} have the lowest observational deviation from CDM indicating little observational difference between the models.

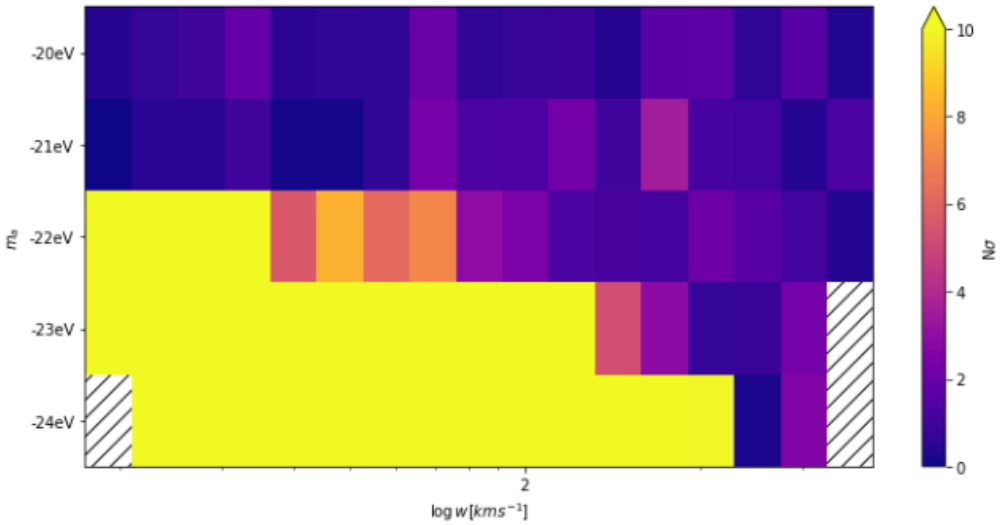

Figure 3.3: Deviations between WALLABY and CDM HIWFs, in factors of observational error. Slashed regions indicate bins that have counts ≤ 5. Universes with ULA mass $m_a = 10^{-20}$ and 10^{-21} have the lowest observational deviation from CDM indicating little observational difference between the models.

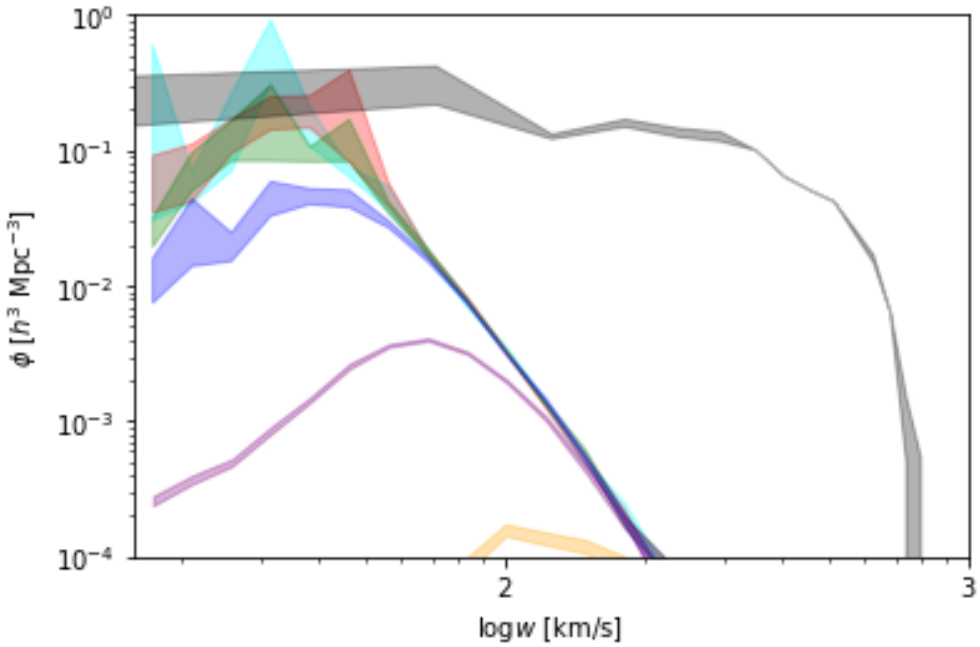

Figure 3.4: Our mock HIWFs compared to the observational ALFALFA HIWF as given by Papastergis et al. (2011). CDM universe is cyan, $m_a = 10^{-20}$ eV universe is red, $m_a = 10^{-21}$ eV universe is green, $m_a = 10^{-22}$ eV universe is blue, $m_a = 10^{-23}$ eV universe is purple, $m_a = 10^{-24}$ universe eV is orange, and observational is black. The contrast in shape is immediately apparent. Furthermore, the observational HIWF covers a greater width range than the simulated universes.

4 Discussion

4.1 The Observational HIWF Against Simulated HIWFs

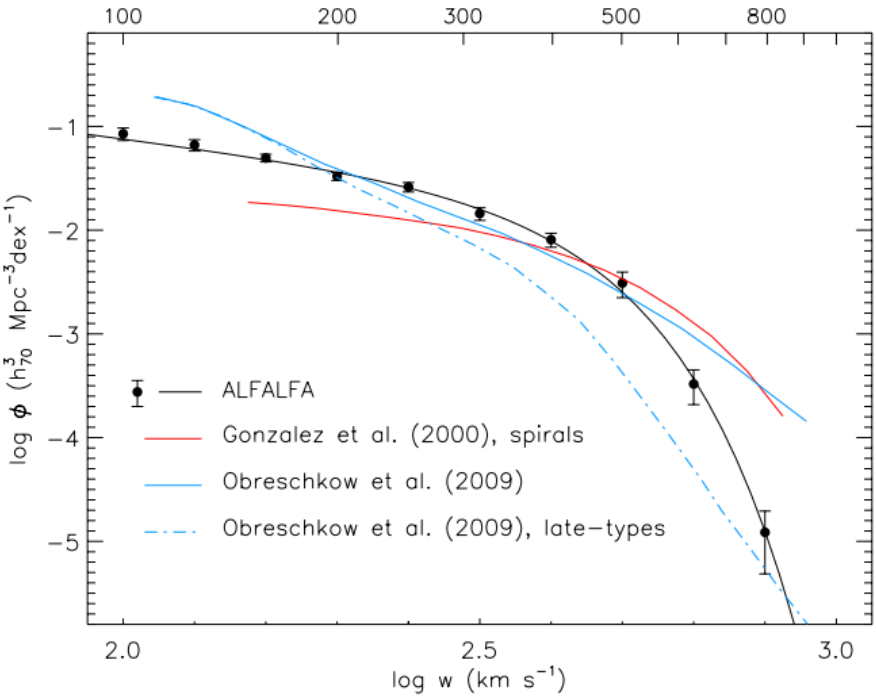

Figure 4.1: The ALFALFA observational HIWF (Papastergis et al., 2011) plotted against simulation outputs. The red line is a HIVF that was produced by the observed luminosity function for spiral galaxies and the Tully-Fisher relationship (Gonzalez et al., 2000). The solid blue line is the original HIWF output of (Obreschkow et al., 2009); note the power law shape that is in disagreement with observation at high widths. The dashed blue is the late-type corrected HIWF that better follows the observational HIWF (Zwaan et al., 2010).

Analyzing the shapes of each HIWF from Figure 3.1, its immediately apparent that they follow power laws. This is consistent with the analytical formula used to generate the rotational velocities for each dark matter halo in the simulation. Specifically, rotational

velocity is assigned according to Equation 2.3, which follows a simple power law. As mentioned previously, this is in contrast to the expected Shchechter shape that is seen with observational HIWFs. This difference is illustrated in Figure 3.4. Notably, simulated HIWFs that follow power laws are not uncommon. Obreschkow et al. (2009) constructed a simulated power-law-shaped HIWF based on the semi-analytic galaxy catalogue created by De Lucia and Blaizot (2007), which itself is based on the Millennium N-body simulation (Springel et al., 2005). Zwaan et al. (2010) argued that this HIWF over-simulated the HI content of massive early-type, i.e. older elliptical, galaxies. Limiting the sample to just late-type galaxies, i.e. spiral, or irregular, young, and star forming galaxies, they were able to recover the luminosity function shape that was in better agreement with the HIPASS survey's observational HIWF. The results of these studies can be seen in Figure 4.1. The simulations in these studies utilized CDM N-body simulations along with analytical expressions for modeling galactic gas physics, star formation, supernovae, and active galaxy nuclei (AGN) feedback. These mechanisms are beyond the scope of this paper's simulation. Thus, differentiating between late-type and early-type galaxies in attempt to smooth the simulated HIWFs in Figure 3.1 isn't feasible. Regardless, it is still interesting to analyze the simulated universes to test ULA masses, especially in the low-width regime where halo number density suppression is of the question.

Notably, there appears to be an under prediction in the simulated number density of low width halos resulting from an over correction in the V_{max} weighting. Figure 4.2 could explain this phenomena. At lower widths, the mock surveys are able to only observe the most face-on, brightest galaxies. This leads to an over estimation in the number of bright low width halos and an under representation of the number of edge-on and dim low width galaxies. As a result, the number density is over corrected when we performed the V_{max} weighting.

4.2 HIWF Deviations

Figures 3.2 and 3.3 visualize the discrepancy between the simulated CDM HIWF and various simulated ULA HIWFs. It can be seen for ALFALFA that any ULA mass greater than or equal to 10^{-21} eV shows little deviation from CDM.DM models with axion masses in this range are observationally indiscernible from CDM models. Similarly, for WALLABY, any mass greater than 10^{-22} eV also exhibit minimal deviation and thus are observationally indistinguishable from CDM.

For ALFALFA, Garland et al. (2024) cites any axion mass greater than approximately 10^{-23} eV and 10^{-22} eV for WALLABY as observationally indistinguishable from CDM. Notably, Garland et al. (2024) utilize HIMFs instead of HIWFs.

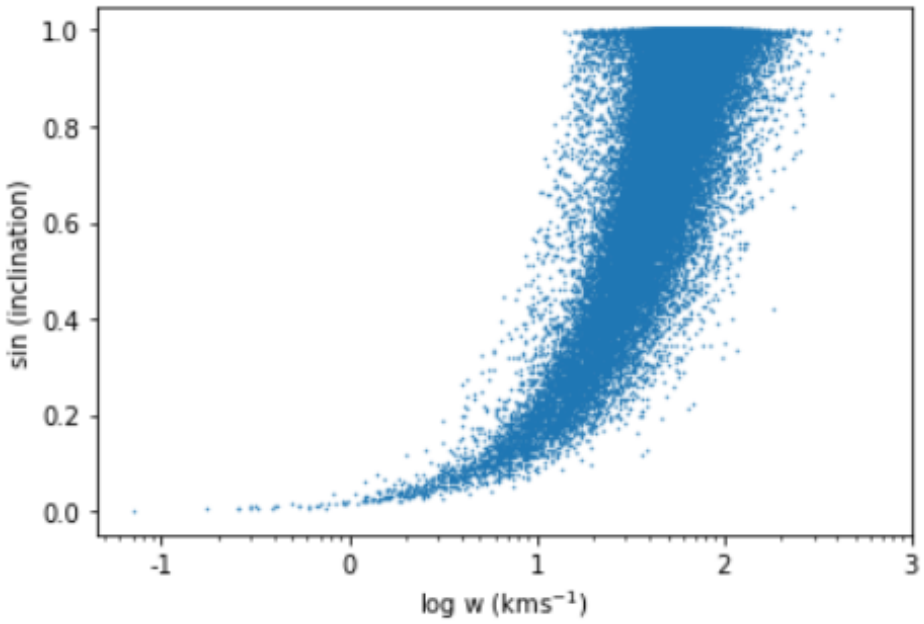

Figure 4.2: Widths plotted against sin(inclination) for ALFALFA. Only the most face-on galaxies are able to be observed in the low width regime (specifically $w \leq 30$ kms^{-1}), leading to the over correction in Vmax

4.3 Conclusion

The purpose of this work was to explore and test the ULA as a potential dark matter particle. Fuzzy dark matter and the ULA in particular present a potential solution to the MSP, a discrepancy in existing CDM models. We make use of six simulated universes, one with CDM as the DM model and five with ULA DM models, each varying the mass of the axion (Garland et al., 2024). We performed mock observations in each survey according to existing survey detection limits, namely ALFALFA and WALLABY. We constructed HIWFs for each universe to test the ULA model against CDM as well as observational data. We find that at the lower width regime, the simulation is only capable of observing only the most face-on galaxies leading to an underprediction in volume number density. At the larger width regime, any ULA mass less than 10^{-22} eV deviates significantly enough from CDM such that it would be observationally noticeable. While both the simulations and the analysis were robust, its possible, if not likely, that future work that amends how widths are calculated by taking into account HI spatial distributions, and an improved halo mass to rotational velocity relationship (perhaps one that is more phenomenological) could go great strives in producing comparisons that are more representative.

5 Acknowledgements

I would like to acknowledge James Garland for his foundational help and advice throughout the research and drafting process, as well as providing me with all the simulated data and supplemental code. My topic has been adapted from his paper (Garland et al., 2024). I also would like to acknowledge Prof. Karen Masters and Prof. Daniel Grin for their invaluable guidance and advice.

Bibliography

P. A. R. Ade, N. Aghanim, Z. Ahmed, R. W. Aikin, K. D. Alexander, M. Arnaud, J. Aumont, C. Baccigalupi, A. J. Banday, D. Barkats, R. B. Barreiro, J. G. Bartlett, N. Bartolo, E. Battaner, K. Benabed, A. Benoît, A. Benoit-Lévy, S. J. Benton, J.-P. Bernard, M. Bersanelli, P. Bielewicz, C. A. Bischoff, J. J. Bock, A. Bonaldi, L. Bonavera, J. R. Bond, J. Borrill, F. R. Bouchet, F. Boulanger, J. A. Brevik, M. Bucher, I. Buder, E. Bullock, C. Burigana, R. C. Butler, V. Buza, E. Calabrese, J.-F. Cardoso, A. Catalano, A. Challinor, R.-R. Chary, H. C. Chiang, P. R. Christensen, L. P. L. Colombo, C. Combet, J. Connors, F. Couchot, A. Coulais, B. P. Crill, A. Curto, F. Cuttaia, L. Danese, R. D. Davies, R. J. Davis, P. de Bernardis, A. de Rosa, G. de Zotti, J. Delabrouille, J.-M. Delouis, F.-X. Désert, C. Dickinson, J. M. Diego, H. Dole, S. Donzelli, O. Doré, M. Douspis, C. D. Dowell, L. Duband, A. Ducout, J. Dunkley, X. Dupac, C. Dvorkin, G. Efstathiou, F. Elsner, T. A. Enßlin, H. K. Eriksen, E. Falgarone, J. P. Filippini, F. Finelli, S. Fliescher, O. Forni, M. Frailis, A. A. Fraisse, E. Franceschi, A. Frejsel, S. Galeotta, S. Galli, K. Ganga, T. Ghosh, M. Giard, E. Gjerløw, S. R. Golwala, J. González-Nuevo, K. M. Górski, S. Gratton, A. Gregorio, A. Gruppuso, J. E. Gudmundsson, M. Halpern, F. K. Hansen, D. Hanson, D. L. Harrison, M. Hasselfield, G. Helou, S. Henrot-Versillé, D. Herranz, S. R. Hildebrandt, G. C. Hilton, E. Hivon, M. Hobson, W. A. Holmes, W. Hovest, V. V. Hristov, K. M. Huffenberger, H. Hui, G. Hurier, K. D. Irwin, A. H. Jaffe, T. R. Jaffe, J. Jewell, W. C. Jones, M. Juvela, A. Karakci, K. S. Karkare, J. P. Kaufman, B. G. Keating, S. Kefeli, E. Keihänen, S. A. Kernasovskiy, R. Keskitalo, T. S. Kisner, R. Kneissl, J. Knoche, L. Knox, J. M. Kovac, N. Krachmalnicoff, M. Kunz, C. L. Kuo, H. Kurki-Suonio, G. Lagache, A. Lähteenmäki, J.-M. Lamarre, A. Lasenby, M. Lattanzi, C. R. Lawrence, E. M. Leitch, R. Leonardi, F. Levrier, A. Lewis, M. Liguori, P. B. Lilje, M. Linden-Vørnle, M. López-Caniego, P. M. Lubin, M. Lueker, J. F. Macías-Pérez, B. Maffei, D. Maino, N. Mandolesi, A. Mangilli, M. Maris, P. G. Martin, E. Martínez-González, S. Masi, P. Mason, S. Matarrese, K. G. Megerian, P. R. Meinhold, A. Melchiorri, L. Mendes, A. Mennella, M. Migliaccio, S. Mitra, M.-A. Miville-Deschênes, A. Moneti, L. Montier, G. Morgante, D. Mortlock, A. Moss, D. Munshi, J. A. Murphy, P. Naselsky, F. Nati, P. Natoli, C. B. Netterfield, H. T. Nguyen, H. U. Nørgaard-Nielsen, F. Noviello, D. Novikov, I. Novikov, R. O'Brient, R. W. Ogburn, A. Orlando, L. Pagano, F. Pajot, R. Paladini, D. Paoletti, B. Partridge, F. Pasian, G. Patanchon, T. J. Pearson, O. Perdereau, L. Perotto, V. Pettorino, F. Piacentini, M. Piat,

D. Pietrobon, S. Plaszczynski, E. Pointecouteau, G. Polenta, N. Ponthieu, G. W. Pratt, S. Prunet, C. Pryke, J.-L. Puget, J. P. Rachen, W. T. Reach, R. Rebolo, M. Reinecke, M. Remazeilles, C. Renault, A. Renzi, S. Richter, I. Ristorcelli, G. Rocha, M. Rossetti, G. Roudier, M. Rowan-Robinson, J. A. Rubiño Martín, B. Rusholme, M. Sandri, D. Santos, M. Savelainen, G. Savini, R. Schwarz, D. Scott, M. D. Seiffert, C. D. Sheehy, L. D. Spencer, Z. K. Staniszewski, V. Stolyarov, R. Sudiwala, R. Sunyaev, D. Sutton, A.-S. Suur-Uski, J.-F. Sygnet, J. A. Tauber, G. P. Teply, L. Terenzi, K. L. Thompson, L. Toffolatti, J. E. Tolan, M. Tomasi, M. Tristram, M. Tucci, A. D. Turner, L. Valenziano, J. Valiviita, B. Van Tent, L. Vibert, P. Vielva, A. G. Vieregg, F. Villa, L. A. Wade, B. D. Wandelt, R. Watson, A. C. Weber, I. K. Wehus, M. White, S. D. M. White, J. Willmert, C. L. Wong, K. W. Yoon, D. Yvon, A. Zacchei, and A. Zonca. Joint analysis of bicep2/keck array and planck data. *Phys. Rev. Lett.*, 114:101301, Mar 2015. doi: 10.1103/PhysRevLett.114.101301. URL https://link.aps.org/doi/10.1103/PhysRevLett.114.101301.

P. A. R. Ade, N. Aghanim, M. Arnaud, M. Ashdown, J. Aumont, C. Baccigalupi, A. J. Banday, R. B. Barreiro, J. G. Bartlett, N. Bartolo, E. Battaner, R. Battye, K. Benabed, A. Benoît, A. Benoit-Lévy, J.-P. Bernard, M. Bersanelli, P. Bielewicz, J. J. Bock, A. Bonaldi, L. Bonavera, J. R. Bond, J. Borrill, F. R. Bouchet, F. Boulanger, M. Bucher, C. Burigana, R. C. Butler, E. Calabrese, J.-F. Cardoso, A. Catalano, A. Challinor, A. Chamballu, R.-R. Chary, H. C. Chiang, J. Chluba, P. R. Christensen, S. Church, D. L. Clements, S. Colombi, L. P. L. Colombo, C. Combet, A. Coulais, B. P. Crill, A. Curto, F. Cuttaia, L. Danese, R. D. Davies, R. J. Davis, P. de Bernardis, A. de Rosa, G. de Zotti, J. Delabrouille, F.-X. Désert, E. Di Valentino, C. Dickinson, J. M. Diego, K. Dolag, H. Dole, S. Donzelli, O. Doré, M. Douspis, A. Ducout, J. Dunkley, X. Dupac, G. Efstathiou, F. Elsner, T. A. Enßlin, H. K. Eriksen, M. Farhang, J. Fergusson, F. Finelli, O. Forni, M. Frailis, A. A. Fraisse, E. Franceschi, A. Frejsel, S. Galeotta, S. Galli, K. Ganga, C. Gauthier, M. Gerbino, T. Ghosh, M. Giard, Y. Giraud-Héraud, E. Giusarma, E. Gjerløw, J. González-Nuevo, K. M. Górski, S. Gratton, A. Gregorio, A. Gruppuso, J. E. Gudmundsson, J. Hamann, F. K. Hansen, D. Hanson, D. L. Harrison, G. Helou, S. Henrot-Versillé, C. Hernández-Monteagudo, D. Herranz, S. R. Hildebrandt, E. Hivon, M. Hobson, W. A. Holmes, A. Hornstrup, W. Hovest, Z. Huang, K. M. Huffenberger, G. Hurier, A. H. Jaffe, T. R. Jaffe, W. C. Jones, M. Juvela, E. Keihänen, R. Keskitalo, T. S. Kisner, R. Kneissl, J. Knoche, L. Knox, M. Kunz, H. Kurki-Suonio, G. Lagache, A. Lähteenmäki, J.-M. Lamarre, A. Lasenby, M. Lattanzi, C. R. Lawrence, J. P. Leahy, R. Leonardi, J. Lesgourgues, F. Levrier, A. Lewis, M. Liguori, P. B. Lilje, M. Linden-Vørnle, M. López-Caniego, P. M. Lubin, J. F. Macías-Pérez, G. Maggio, D. Maino, N. Mandolesi, A. Mangilli, A. Marchini, M. Maris, P. G. Martin, M. Martinelli, E. Martínez-González, S. Masi, S. Matarrese, P. McGehee, P. R. Meinhold, A. Melchiorri, J.-B. Melin, L. Mendes, A. Mennella, M. Migli-

accio, M. Millea, S. Mitra, M.-A. Miville-Deschênes, A. Moneti, L. Montier, G. Morgante, D. Mortlock, A. Moss, D. Munshi, J. A. Murphy, P. Naselsky, F. Nati, P. Natoli, C. B. Netterfield, H. U. Nørgaard-Nielsen, F. Noviello, D. Novikov, I. Novikov, C. A. Oxborrow, F. Paci, L. Pagano, F. Pajot, R. Paladini, D. Paoletti, B. Partridge, F. Pasian, G. Patanchon, T. J. Pearson, O. Perdereau, L. Perotto, F. Perrotta, V. Pettorino, F. Piacentini, M. Piat, E. Pierpaoli, D. Pietrobon, S. Plaszczynski, E. Pointecouteau, G. Polenta, L. Popa, G. W. Pratt, G. Prézeau, S. Prunet, J.-L. Puget, J. P. Rachen, W. T. Reach, R. Rebolo, M. Reinecke, M. Remazeilles, C. Renault, A. Renzi, I. Ristorcelli, G. Rocha, C. Rosset, M. Rossetti, G. Roudier, B. Rouillé d'Orfeuil, M. Rowan-Robinson, J. A. Rubiño-Martín, B. Rusholme, N. Said, V. Salvatelli, L. Salvati, M. Sandri, D. Santos, M. Savelainen, G. Savini, D. Scott, M. D. Seiffert, P. Serra, E. P. S. Shellard, L. D. Spencer, M. Spinelli, V. Stolyarov, R. Stompor, R. Sudiwala, R. Sunyaev, D. Sutton, A.-S. Suur-Uski, J.-F. Sygnet, J. A. Tauber, L. Terenzi, L. Toffolatti, M. Tomasi, M. Tristram, T. Trombetti, M. Tucci, J. Tuovinen, M. Türler, G. Umana, L. Valenziano, J. Valiviita, F. Van Tent, P. Vielva, F. Villa, L. A. Wade, B. D. Wandelt, I. K. Wehus, M. White, S. D. M. White, A. Wilkinson, D. Yvon, A. Zacchei, and A. Zonca. Planck2015 results: Xiii. cosmological parameters. *Astronomy amp; Astrophysics*, 594:A13, September 2016. ISSN 1432-0746. doi: 10.1051/0004-6361/201525830. URL http://dx.doi.org/10.1051/0004-6361/201525830.

K. Aditya, Peter Kamphuis, Arunima Banerjee, Sviatoslav Borisov, Aleksandr Mosenkov, Aleksandra Antipova, and Dmitry Makarov. H I 21 cm observation and mass models of the extremely thin galaxy FGC 1440. , 509(3):4071–4093, January 2022. doi: 10.1093/mnras/stab3143.

C. S. Beals. On the Interpretation of Interstellar Lines. *Monthly Notices of the Royal Astronomical Society*, 96(7):661–678, 05 1936. ISSN 0035-8711. doi: 10.1093/mnras/96.7.661. URL https://doi.org/10.1093/mnras/96.7.661.

K. G. Begeman. HI rotation curves of spiral galaxies. I. NGC 3198. , 223:47–60, October 1989.

C. L. Bennett, M. Halpern, G. Hinshaw, N. Jarosik, A. Kogut, M. Limon, S. S. Meyer, L. Page, D. N. Spergel, G. S. Tucker, E. Wollack, E. L. Wright, C. Barnes, M. R. Greason, R. S. Hill, E. Komatsu, M. R. Nolta, N. Odegard, H. V. Peiris, L. Verde, and J. L. Weiland. First-year wilkinson microwave anisotropy probe (wmap) observations: Preliminary maps and basic results. *The Astrophysical Journal Supplement Series*, 148(1):1–27, September 2003. ISSN 1538-4365. doi: 10.1086/377253. URL http://dx.doi.org/10.1086/377253.

Michael Boylan-Kolchin, Volker Springel, Simon D. M. White, Adrian Jenkins, and Gerard

Lemson. Resolving cosmic structure formation with the Millennium-II Simulation. , 398(3):1150–1164, September 2009. doi: 10.1111/j.1365-2966.2009.15191.x.

Margot M. Brouwer, Manus R. Visser, Andrej Dvornik, Henk Hoekstra, Konrad Kuijken, Edwin A. Valentijn, Maciej Bilicki, Chris Blake, Sarah Brough, Hugo Buddelmeijer, Thomas Erben, Catherine Heymans, Hendrik Hildebrandt, Benne W. Holwerda, Andrew M. Hopkins, Dominik Klaes, Jochen Liske, Jon Loveday, John McFarland, Reiko Nakajima, Cristóbal Sifón, and Edward N. Taylor. First test of verlinde's theory of emergent gravity using weak gravitational lensing measurements. *Monthly Notices of the Royal Astronomical Society*, 466(3):2547–2559, December 2016. ISSN 1365-2966. doi: 10.1093/mnras/stw3192. URL http://dx.doi.org/10.1093/mnras/stw3192.

B. J. Carr, Kazunori Kohri, Yuuiti Sendouda, and Jun'ichi Yokoyama. New cosmological constraints on primordial black holes. *Physical Review D*, 81(10), May 2010. ISSN 1550-2368. doi: 10.1103/physrevd.81.104019. URL http://dx.doi.org/10.1103/PhysRevD.81.104019.

Marc Davis, F. J. Summers, and David Schlegel. Large-scale structure in a universe with mixed hot and cold dark matter. , 359(6394):393–396, October 1992. doi: 10.1038/359393a0.

Gabriella De Lucia and Jérémy Blaizot. The hierarchical formation of the brightest cluster galaxies. *Monthly Notices of the Royal Astronomical Society*, 375(1):2–14, 01 2007. ISSN 0035-8711. doi: 10.1111/j.1365-2966.2006.11287.x. URL https://doi.org/10.1111/j.1365-2966.2006.11287.x.

Avishai Dekel and Joseph Silk. The origin of dwarf galaxies, cold dark matter, and biased galaxy formation. *Astrophysical Journal, Part 1 (ISSN 0004-637X), vol. 303, April 1, 1986, p. 39-55.*, 303:39–55, 1986.

Michael Dine, Willy Fischler, and Mark Srednicki. A simple solution to the strong cp problem with a harmless axion. *Physics Letters B*, 104(3):199–202, 1981. ISSN 0370-2693. doi: https://doi.org/10.1016/0370-2693(81)90590-6. URL https://www.sciencedirect.com/science/article/pii/0370269381905906.

Xiaolong Du, Christoph Behrens, and Jens C. Niemeyer. Substructure of fuzzy dark matter haloes. *Monthly Notices of the Royal Astronomical Society*, 465(1):941–951, 10 2016. ISSN 0035-8711. doi: 10.1093/mnras/stw2724. URL https://doi.org/10.1093/mnras/stw2724.

Carlos S. Frenk, August E. Evrard, Simon D. M. White, and F. J. Summers. Galaxy dynamics in clusters. *The Astrophysical Journal*, 472(2):460, dec 1996. doi: 10.1086/178079. URL https://dx.doi.org/10.1086/178079.

James T. Garland, Karen L. Masters, and Daniel Grin. Using hi observations of low-mass galaxies to test ultra-light axion dark matter, 2024.

G. W. Gibbons and S. W. Hawking. Cosmological event horizons, thermodynamics, and particle creation. *Phys. Rev. D*, 15:2738–2751, May 1977. doi: 10.1103/PhysRevD.15.2738. URL https://link.aps.org/doi/10.1103/PhysRevD.15.2738.

Anthony H. Gonzalez, Kurtis A. Williams, James S. Bullock, Tsafrir S. Kolatt, and Joel R. Primack. The velocity function of galaxies. *The Astrophysical Journal*, 528(1):145–155, January 2000. ISSN 1538-4357. doi: 10.1086/308159. URL http://dx.doi.org/10.1086/308159.

Martha P. Haynes, Riccardo Giovanelli, Brian R. Kent, Elizabeth A. K. Adams, Thomas J. Balonek, David W. Craig, Derek Fertig, Rose Finn, Carlo Giovanardi, Gregory Hallenbeck, Kelley M. Hess, G. Lyle Hoffman, Shan Huang, Michael G. Jones, Rebecca A. Koopmann, David A. Kornreich, Lukas Leisman, Jeffrey Miller, Crystal Moorman, Jessica O'Connor, Aileen O'Donoghue, Emmanouil Papastergis, Parker Troischt, David Stark, and Li Xiao. The arecibo legacy fast alfa survey: The alfalfa extragalactic h i source catalog. *The Astrophysical Journal*, 861(1):49, jul 2018. doi: 10.3847/1538-4357/aac956. URL https://dx.doi.org/10.3847/1538-4357/aac956.

Wayne Hu, Rennan Barkana, and Andrei Gruzinov. Fuzzy cold dark matter: The wave properties of ultralight particles. *Phys. Rev. Lett.*, 85:1158–1161, Aug 2000. doi: 10.1103/PhysRevLett.85.1158. URL https://link.aps.org/doi/10.1103/PhysRevLett.85.1158.

Jai-chan Hwang and Hyerim Noh. Axion as a cold dark matter candidate. *Physics Letters B*, 680(1):1–3, September 2009. ISSN 0370-2693. doi: 10.1016/j.physletb.2009.08.031. URL http://dx.doi.org/10.1016/j.physletb.2009.08.031.

A. Jenkins, C. S. Frenk, S. D. M. White, J. M. Colberg, S. Cole, A. E. Evrard, H. M. P. Couchman, and N. Yoshida. The mass function of dark matter haloes. , 321(2):372–384, February 2001. doi: 10.1046/j.1365-8711.2001.04029.x.

Michael G Jones, Martha P Haynes, Riccardo Giovanelli, and Crystal Moorman. The alfalfa hi mass function: a dichotomy in the low-mass slope and a locally suppressed 'knee' mass. *Monthly Notices of the Royal Astronomical Society*, 477(1):2–17, February 2018.

ISSN 1365-2966. doi: 10.1093/mnras/sty521. URL http://dx.doi.org/10.1093/mnras/sty521.

Harley Katz, Harry Desmond, Stacy McGaugh, and Federico Lelli. The tight empirical relation between dark matter halo mass and flat rotation velocity for late-type galaxies. , 483(1):L98–L103, February 2019. doi: 10.1093/mnrasl/sly203.

Jihn E. Kim. Weak-interaction singlet and strong CP invariance. *Phys. Rev. Lett.*, 43:103–107, Jul 1979. doi: 10.1103/PhysRevLett.43.103. URL https://link.aps.org/doi/10.1103/PhysRevLett.43.103.

Anatoly Klypin, Andrey V. Kravtsov, Octavio Valenzuela, and Francisco Prada. Where Are the Missing Galactic Satellites? , 522(1):82–92, September 1999. doi: 10.1086/307643.

Bärbel S. Koribalski, L. Staveley-Smith, T. Westmeier, P. Serra, K. Spekkens, O. I. Wong, K. Lee-Waddell, C. D. P. Lagos, D. Obreschkow, E. V. Ryan-Weber, M. Zwaan, V. Kilborn, G. Bekiaris, K. Bekki, F. Bigiel, A. Boselli, A. Bosma, B. Catinella, G. Chauhan, M. E. Cluver, M. Colless, H. M. Courtois, R. A. Crain, W. J. G. de Blok, H. Dénes, A. R. Duffy, A. Elagali, C. J. Fluke, B. Q. For, G. Heald, P. A. Henning, K. M. Hess, B. W. Holwerda, C. Howlett, T. Jarrett, D. H. Jones, M. G. Jones, G. I. G. Józsa, R. Jurek, E. Jütte, P. Kamphuis, I. Karachentsev, J. Kerp, D. Kleiner, R. C. Kraan-Korteweg, Á. R. López-Sánchez, J. Madrid, M. Meyer, J. Mould, C. Murugeshan, R. P. Norris, S. H. Oh, T. A. Oosterloo, A. Popping, M. Putman, T. N. Reynolds, J. Rhee, A. S. G. Robotham, S. Ryder, A. C. Schröder, Li Shao, A. R. H. Stevens, E. N. Taylor, J. M. vanÂ der Hulst, L. Verdes-Montenegro, B. P. Wakker, J. Wang, M. Whiting, B. Winkel, and C. Wolf. WALLABY - an SKA Pathfinder HI survey. , 365(7):118, July 2020. doi: 10.1007/s10509-020-03831-4.

Umberto Maio and Matteo Viel. The first billion years of a warm dark matter universe. , 446(3):2760–2775, January 2015. doi: 10.1093/mnras/stu2304.

David J. E. Marsh. Axion cosmology. , 643:1–79, July 2016. doi: 10.1016/j.physrep.2016.06.005.

Karen L. Masters, Martha P. Haynes, and Riccardo Giovanelli. The impact of distance uncertainties on local luminosity and mass functions. *The Astrophysical Journal*, 607(2): L115, may 2004. doi: 10.1086/422100. URL https://dx.doi.org/10.1086/422100.

Julio F. Navarro. The structure of cold dark matter halos. *Symposium - International Astronomical Union*, 171:255–258, 1996. doi: 10.1017/S0074180900232452.

Dylan Nelson, Volker Springel, Annalisa Pillepich, Vicente Rodriguez-Gomez, Paul Torrey, Shy Genel, Mark Vogelsberger, Ruediger Pakmor, Federico Marinacci, Rainer Weinberger, Luke Kelley, Mark Lovell, Benedikt Diemer, and Lars Hernquist. The illustristng simulations: Public data release, 2021.

D. Obreschkow, D. Croton, G. De Lucia, S. Khochfar, and S. Rawlings. Simulation of the cosmic evolution of atomic and molecular hydrogen in galaxies. *The Astrophysical Journal*, 698(2):1467–1484, June 2009. ISSN 1538-4357. doi: 10.1088/0004-637x/698/2/1467. URL http://dx.doi.org/10.1088/0004-637X/698/2/1467.

Emmanouil Papastergis, Ann M. Martin, Riccardo Giovanelli, and Martha P. Haynes. The velocity width function of galaxies from the 40 *The Astrophysical Journal*, 739(1): 38, sep 2011. doi: 10.1088/0004-637X/739/1/38. URL https://dx.doi.org/10.1088/0004-637X/739/1/38.

Samuel Passaglia and Wayne Hu. Accurate effective fluid approximation for ultralight axions. , 105(12):123529, June 2022. doi: 10.1103/PhysRevD.105.123529.

R. D. Peccei and Helen R. Quinn. CP conservation in the presence of pseudoparticles. *Phys. Rev. Lett.*, 38:1440–1443, Jun 1977. doi: 10.1103/PhysRevLett.38.1440. URL https://link.aps.org/doi/10.1103/PhysRevLett.38.1440.

Annika H. G. Peter. Dark matter: A brief review, 2012.

William H. Press and Paul Schechter. Formation of Galaxies and Clusters of Galaxies by Self-Similar Gravitational Condensation. , 187:425–438, February 1974. doi: 10.1086/152650.

V. C. Rubin, Jr. Ford, W. K., and N. Thonnard. Extended rotation curves of high-luminosity spiral galaxies. IV. Systematic dynamical properties, Sa -> Sc. , 225:L107–L111, November 1978. doi: 10.1086/182804.

Maarten Schmidt. Space Distribution and Luminosity Functions of Quasi-Stellar Radio Sources. , 151:393, February 1968. doi: 10.1086/149446.

Ravi K. Sheth and Giuseppe Tormen. An excursion set model of hierarchical clustering: ellipsoidal collapse and the moving barrier. *Monthly Notices of the Royal Astronomical Society*, 329(1):61–75, 01 2002. ISSN 0035-8711. doi: 10.1046/j.1365-8711.2002.04950.x. URL https://doi.org/10.1046/j.1365-8711.2002.04950.x.

Mikhail A. Shifman, A. I. Vainshtein, and Valentin I. Zakharov. Can Confinement Ensure Natural CP Invariance of Strong Interactions? *Nucl. Phys. B*, 166:493–506, 1980. doi: 10.1016/0550-3213(80)90209-6.

Sinclair Smith. The Mass of the Virgo Cluster. , 83:23, January 1936. doi: 10.1086/143697.

David N. Spergel and Paul J. Steinhardt. Observational Evidence for Self-Interacting Cold Dark Matter. , 84(17):3760–3763, April 2000. doi: 10.1103/PhysRevLett.84.3760.

Volker Springel, Simon D. M. White, Adrian Jenkins, Carlos S. Frenk, Naoki Yoshida, Liang Gao, Julio Navarro, Robert Thacker, Darren Croton, John Helly, John A. Peacock, Shaun Cole, Peter Thomas, Hugh Couchman, August Evrard, Jörg Colberg, and Frazer Pearce. Simulations of the formation, evolution and clustering of galaxies and quasars. , 435(7042):629–636, June 2005. doi: 10.1038/nature03597.

Michael S. Turner. Coherent scalar-field oscillations in an expanding universe. *Phys. Rev. D*, 28:1243–1247, Sep 1983. doi: 10.1103/PhysRevD.28.1243. URL https://link.aps.org/doi/10.1103/PhysRevD.28.1243.

Francisco Villaescusa-Navarro, Shy Genel, Emanuele Castorina, Andrej Obuljen, David N. Spergel, Lars Hernquist, Dylan Nelson, Isabella P. Carucci, Annalisa Pillepich, Federico Marinacci, Benedikt Diemer, Mark Vogelsberger, Rainer Weinberger, and Rüdiger Pakmor. Ingredients for 21 cm Intensity Mapping. , 866(2):135, October 2018. doi: 10.3847/1538-4357/aadbao.

Michael S. Warren, Kevork Abazajian, Daniel E. Holz, and Luís Teodoro. Precision Determination of the Mass Function of Dark Matter Halos. , 646(2):881–885, August 2006. doi: 10.1086/504962.

T. Westmeier, N. Deg, K. Spekkens, T. N. Reynolds, A. X. Shen, S. Gaudet, S. Goliath, M. T. Huynh, P. Venkataraman, X. Lin, T. O'Beirne, B. Catinella, L. Cortese, H. Dénes, A. Elagali, B.-Q. For, G. I. G. Józsa, C. Howlett, J. M. van der Hulst, R. J. Jurek, P. Kamphuis, V. A. Kilborn, D. Kleiner, B. S. Koribalski, K. Lee-Waddell, C. Murugeshan, J. Rhee, P. Serra, L. Shao, L. Staveley-Smith, J. Wang, O. I. Wong, M. A. Zwaan, J. R. Allison, C. S. Anderson, Lewis Ball, D. C.-J. Bock, D. Brodrick, J. D. Bunton, F. R. Cooray, N. Gupta, D. B. Hayman, E. K. Mahony, V. A. Moss, A. Ng, S. E. Pearce, W. Raja, D. N. Roxby, M. A. Voronkov, K. A. Warhurst, H. M. Courtois, and K. Said. Wallaby pilot survey: Public release of h <scp>i</scp> data for almost 600 galaxies from phase 1 of askap pilot observations. *Publications of the Astronomical Society of Australia*, 39, 2022. ISSN 1448-6083. doi: 10.1017/pasa.2022.50. URL http://dx.doi.org/10.1017/pasa.2022.50.

Simon D. M. White, Marc Davis, George Efstathiou, and Carlos S. Frenk. Galaxy distribution in a cold dark matter universe. , 330(6147):451–453, December 1987. doi: 10.1038/330451a0.

Harrison Winch, Renee Hlozek, David J. E. Marsh, Daniel Grin, and Keir Rogers. Extreme axions unveiled: a novel fluid approach for cosmological modeling, 2023.

Bing-Lin Young. A survey of dark matter and related topics in cosmology. *Frontiers of Physics*, 12(2):121201, April 2017. doi: 10.1007/s11467-016-0583-4.

Niankun Yu, Luis C. Ho, and Jing Wang. On the determination of rotation velocity and dynamical mass of galaxies based on integrated h i spectra. *The Astrophysical Journal*, 898 (2):102, jul 2020. doi: 10.3847/1538-4357/ab9ac5. URL https://dx.doi.org/10.3847/1538-4357/ab9ac5.

J. Zavala, Y. P. Jing, A. Faltenbacher, G. Yepes, Y. Hoffman, S. Gottlöber, and B. Catinella. The velocity function in the local environment from cdm and wdm constrained simulations. *The Astrophysical Journal*, 700(2):1779, jul 2009. doi: 10.1088/0004-637X/700/2/1779. URL https://dx.doi.org/10.1088/0004-637X/700/2/1779.

A P Zhitnitskii. Possible suppression of axion-hadron interactions. *Sov. J. Nucl. Phys. (Engl. Transl.); (United States)*, 1980. URL https://www.osti.gov/biblio/7063072.

Zhimin Zhou, Hong Wu, Xu Zhou, and Jun Ma. The relation between h i gas and star formation properties in nearby galaxies. *Publications of the Astronomical Society of the Pacific*, 130(991):094101, August 2018. ISSN 1538-3873. doi: 10.1088/1538-3873/aad407. URL http://dx.doi.org/10.1088/1538-3873/aad407.

M. A. Zwaan, M. J. Meyer, L. Staveley-Smith, and R. L. Webster. The HIPASS catalogue: H i and environmental effects on the H i mass function of galaxies. *Monthly Notices of the Royal Astronomical Society: Letters*, 359(1):L30–L34, 05 2005. ISSN 1745-3925. doi: 10.1111/j.1745-3933.2005.00029.x. URL https://doi.org/10.1111/j.1745-3933.2005.00029.x.

M. A. Zwaan, M. J. Meyer, and L. Staveley-Smith. The velocity function of gas-rich galaxies. *Monthly Notices of the Royal Astronomical Society*, 403(4):1969–1977, 04 2010. ISSN 0035-8711. doi: 10.1111/j.1365-2966.2009.16188.x. URL https://doi.org/10.1111/j.1365-2966.2009.16188.x.

F. Zwicky. Die Rotverschiebung von extragalaktischen Nebeln. *Helvetica Physica Acta*, 6: 110–127, January 1933.

F. Zwicky. On the Masses of Nebulae and of Clusters of Nebulae. , 86:217, October 1937. doi: 10.1086/143864.